Oxygen Evolution Catalysts

DOI: 10.1002/anie.201402822

A Strongly Coupled Graphene and FeNi Double Hydroxide Hybrid as an Excellent Electrocatalyst for the Oxygen Evolution Reaction**

*Xia Long, Jinkai Li, Shuang Xiao, Keyou Yan, Zilong Wang, Haining Chen, and Shihe Yang**

Abstract: *Cost-effective electrocatalysts for the oxygen evolution reaction (OER) are critical to energy conversion and storage processes. A novel strategy is used to synthesize a non-noble-metal-based electrocatalyst of the OER by finely combining layered FeNi double hydroxide that is catalytically active and electric conducting graphene sheets, taking advantage of the electrostatic attraction between the two positively charged nanosheets. The synergy between the catalytic activity of the double hydroxide and the enhanced electron transport arising from the graphene resulted in superior electrocatalytic properties of the FeNi-GO hybrids for the OER with overpotentials as low as 0.21 V, which was further reduced to 0.195 V after the reduction treatment. Moreover, the turnover frequency at the overpotential of 0.3 V has reached 1 s^{-1}, which is much higher than those previously reported for non-noble-metal-based electrocatalysts.*

The growing demand for energy and the increasing concerns about environment pollution from fossil fuels are stimulating intense research interest in energy conversion and storage from alternative sustainable energy sources. As one of the most important process to produce and store renewable energy in chemical form, the oxygen evolution reaction (OER) has led to many studies in recent years. However, the kinetics of OER is sluggish. Therefore, an effective electrocatalyst is needed to accelerate the reaction and reduce the large overpotential and thus improve the energy conversion efficiency. Metal oxides are the most active and durable electrocatalysts for OER, among which IrO_2 and RuO_2 are thought to be best OER catalysts in both acidic and alkaline solutions.[1] However, the high cost and element scarcity greatly hindered the widespread use of these noble-metal oxide catalysts. Therefore, it is desirable to develop efficient alternative catalysts based on inexpensive and earth-abundant elements without compromising good catalytic activity and durability for OER. Recently, extensive efforts have been made to use perovskites[2] and first-row transition-metal-based materials[3] as low-cost catalysts or electrode materials for many renewable energy applications. The activities of transition-metal-based catalysts for OER were proposed to relate to the 3d electron number of the transition metal ions, the enthalpy for the lower to higher oxide transition, and the surface oxygen binding energy.[4] Moreover, the surface transition-metal ions whose e_g orbitals could bond with surface-anion adsorbates[5] influence the binding of oxygenic intermediate species and thus the OER activity.[2a] Recently, layered $Ni(OH)_2$/NiOOH was found to be an active catalyst in a study of the in situ structure transformation from NiO to NiOOH, which is in direct parallel with the increasing catalytic activity.[6] Because the layered structure allows the intercalation of water and anions and therefore lend bulk redox activity.[7] Studies on ZnCo layered double hydroxide (LDH) further confirmed that catalysts with such a layered structure had higher activities than Co-based catalysts with other structures.[3d]

Herein, we propose a novel strategy to design an electrocatalytic active catalyst on OER at molecular level, by taking advantage of the electrostatic attraction between two types of oppositely charged nanosheets. One of the starting material is FeNi double hydroxide cation layers that are exfoliated from FeNi LDHs, which is an OER-active material[3c] with exchangeable interlayer anions. The other starting nanosheet is graphene oxide (GO), which is an ideal two-dimensional carbon material with atomic thinness, large surface area, and good electrical conductivity after reduction treatment.[8] Assisted by the electrostatic attraction, the GO nanosheets with multifunctional oxygenic groups are assembled with the cationic FeNi double hydroxide layers in aqueous solution, forming charge balancing interlayers in the resulting hybrid sheets. We show that the as prepared FeNi-GO LDHs exhibit efficient electrocatalytic activity on OER with overpotential as low as 0.21 V and Tafel slope around 40 mV/dec. Furthermore, after the reduction of FeNi-GO LDH to FeNi-rGO LDH, the overpotential of OER was further decreased to 0.195 V and the turnover frequency (TOF) reached 0.98 s^{-1} at the overpotential of 0.3 V, a superior OER catalytic performance unmatched by other FeNi compounds reported to date.

FeNi-CO_3 LDH nanoplates with a lateral size of around 300 nm (Figure 1 B,E) were synthesized by a simple hydrothermal method (see the Supporting Information for details). Because the carbonate ions have a rather high affinity to the hydroxide layers of LDHs and thus are quite difficult to delaminate,[9] a decarbonation process was carried out in a HCl and NaCl mixed solution[9b,10] to convert FeNi-CO_3 LDH into FeNi-Cl LDH, which could be more easily delaminated. Following that, the FeNi-Cl LDH precursors were dispersed in a GO aqueous suspension, and the resulting mixture was magnetically stirred for ten days to ensure

[*] X. Long, J. Li, S. Xiao, K. Yan, Z. Wang, H. Chen, S. Yang
Department of Chemistry
William Mong Institute of Nano Science and Technology
The Hong Kong University of Science and Technology
Clear Water Bay, Kowloon (Hong Kong)
E-mail: chsyang@ust.hk

[**] This work was supported by the HK-RGC General Research Funds (HKUST 606511 and 605710).

Supporting information for this article is available on the WWW under http://dx.doi.org/10.1002/anie.201402822.

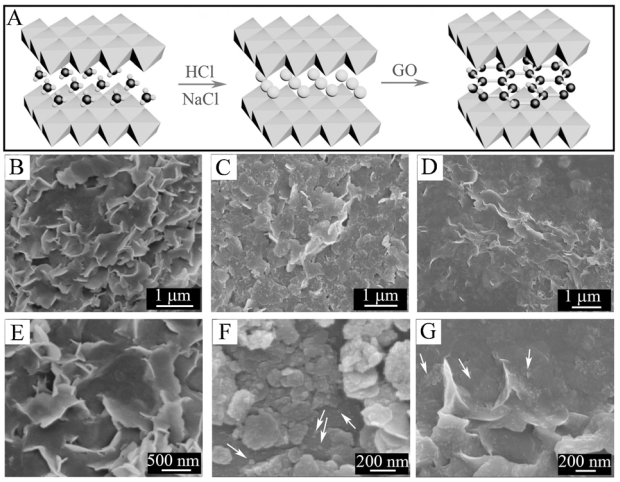

Figure 1. Synthesis and SEM images of FeNi LDH with different anions. A) Fabrication process of FeNi-GO LDHs: FeNi-CO_3 LDHs were dispersed in a HCl and NaCl mixed solution and transformed into FeNi-Cl LDHs, which were further transformed into FeNi-GO LDH hybrid by the anion exchange process. B–G) SEM images of as-prepared FeNi-CO_3 LDHs (B, E), FeNi-Cl LDHs (C, F), and FeNi-GO LDHs (D, G) at different magnifications (arrows point at small nanoplates).

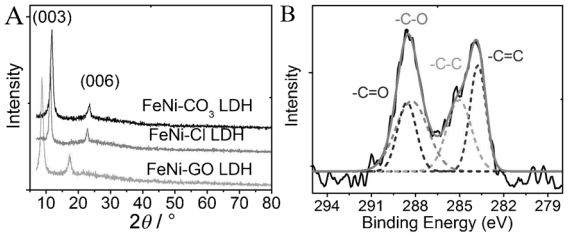

Figure 2. XRD and XPS spectra of FeNi LDHs. A) XRD patterns of FeNi LDH with different charge balancing anions. B) C 1s XPS spectrum of the FeNi-GO LDH hybrid with multi-peak fitting deconvolution. Black curve: real spectrum; gray curve: the sum of fitting curves (dashed lines: fitted curves).

maximal exfoliation of LDHs and assembly of GO with exfoliated FeNi double hydroxide layers (Figure 1 A). Figure 1 B–G show that all of the as-prepared LDHs with different interlayer anions have a nanoplate morphology, indicating the structural preservation after the anion exchange processes. However, the surfaces of the nanoplates became rough, and many smaller nanoplates (see white arrows) appeared from the SEM images of FeNi-Cl LDHs (Figure 1 C,F) and FeNi-GO LDHs (Figure 1 D,G). TEM images confirmed the existence of smaller nanoplates (Supporting Information, Figure S1A), which appear to be exfoliated FeNi-Cl LDHs based on the crystal lattice distance of 0.78 nm that could be indexed as (003) of FeNi LDH (Supporting Information, Figure S1B). Flexible GO sheets could be seen at the edge of FeNi-GO LDH (Supporting Information, Figure S2).

X-ray diffraction (XRD), which is one of the most important technique to estimate the exfoliation, decarbonization and ion exchange of LDHs, gives the direct information of basal spacings of LDHs along the *c* axis and is widely used in determining the structure of layered materials.[9b,10,11] As shown in Figure 2 A, XRD patterns of the starting LDHs and the restacked hybrid materials are largely consistent with the standard XRD pattern of FeNi LDH but with peaks being shifted. The two sharp and strong diffraction peaks indexed as (003) and (006) are shifted to lower 2θ values after the anion exchange processes. The reflection peak shifts are translated to the basal spacings (BS) of FeNi-CO_3 LDH and FeNi-Cl LDH along the *c* axis at about 0.75 nm and about 0.78 nm, respectively. The interlayer expansion is in line with previous studies reported in the literature.[9b,10] More interestingly, the (003) diffraction peak of FeNi-GO LDH appears at 7.8°, corresponding to a large increase of the BS value to 1.1 nm. This value was further confirmed by atomic force microscopic (AFM) images in the Supporting Information, Figure S3, and is actually in good agreement with the summing thickness of one layer of FeNi double hydroxide (ca. 0.46 nm) and one layer of GO (ca. 0.7 nm; Supporting Information, Figure S3). As a result, the picture emerges that the assembled product has essentially a heterostructure comprising the FeNi double hydroxide and GO layers stacked in alternation along the *c* axis. Energy dispersive X-ray spectroscopy (EDX; Supporting Information, Figure S4) further confirmed the layered hybrid composed of Fe, Ni, C, and O, while C comes from GO, indicating that the GO nanosheets and FeNi double hydroxides coexist in the formed plate-like LDHs. A typical survey scan X-ray photoelectron spectrum (XPS) of the FeNi-GO LDH is shown in the Supporting Information, Figure S5A, which reveals the existence of both Fe and Ni in the as synthesized hybrid. The Fe species was found to be mostly in the +3 oxidation state according to the high-resolution Fe 2p XPS spectrum (Supporting Information, Figure S5B). Figure 2 B shows the C 1s core level spectrum together with the deconvolution analysis result. The spectrum divulges the distribution of the C atoms with different electronic environments in the FeNi-GO LDH hybrid, including carboxyl groups (288.9 eV), C=O groups (287.8 eV), sp^3-hybridized saturated carbon species (285.0 eV), and sp^2-hybridized graphitic carbons (284.5 eV), in keeping with the results reported previously.[12]

Electrocatalytic properties of the FeNi-GO LDH hybrid were investigated with respect to OER in a typical three-electrode configuration in 1 M KOH. Ni foam uniformly coated with the as-synthesized FeNi-GO LDH hybrid was used as the working electrode. For comparison, three reference samples were also tested under otherwise identical conditions, and they include FeNi LDH nucleated and grown on GO (labeled as FeNi LDH/GO), which was previously reported to be an advanced electrode material,[3c] physical mixture of FeNi LDH and GO (labeled as FeNi LDH + GO), and FeNi LDH without GO (simply labeled as FeNi LDH). The *iR*-corrected linear sweep voltammetry (LSV) curves of OERs for the set of catalysts are shown in Figure 3 A. Apart from an additional electron-transfer process at around 1.38 V, which can be assigned to the $Ni^{II}/Ni^{III\ or\ IV}$ redox couple, several features are worth noting. First, the OER onset potentials and thus the overpotentials for these catalysts are close to each other (Figure 3 A,B): FeNi-GO LDH (1.44 V),

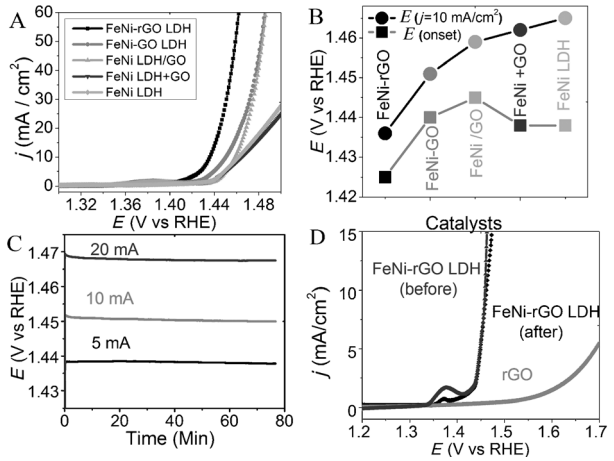

Figure 3. Electrochemical performance of the FeNi LDH-based catalysts on OER. A) *iR*-corrected polarization curves of FeNi-rGO LDH, FeNi-GO LDH, FeNi LDH/GO, FeNi LDH + GO, and FeNi LDH on Ni foam electrodes in 1 M KOH; B) onset potentials (E_{onset}) and potentials required to reach $j = 10\ mA\,cm^{-2}$ ($E_{j=10\ mA\,cm^{-2}}$) of the OER catalyzed by prepared catalysts; C) chronopotentiometry curves of the FeNi-rGO LDH on Ni foam electrode under high current densities of 5, 10, and 20 $mA\,cm^{-2}$; D) LSV curves of rGO and FeNi-rGO LDH before and after chronopotentiometry measurement at a current density of 10 $mA\,cm^{-2}$ for about 8 h. All of the measurements were conducted with a catalyst loading of 0.25 $mg\,cm^{-2}$.

FeNi LDH/GO (1.438 V), FeNi LDH + GO (1.445 V), and FeNi LDH (1.438 V); these values are also close to the reported overpotential of OER catalyzed by FeNi LDH/CNT hybrid.[3c] This result seems to be mainly dictated by the similar catalytically active center in these catalysts. Second, FeNi-GO LDH is reckoned to be the most active catalyst among the four samples; the corresponding current gradually rises at around 1.41 V until picking up sharply rise at 1.44 V (the onset potential), indicating the start of water oxidation. Despite the similar OER overpotentials of the four catalysts, the FeNi-GO LDH hybrid can attain the highest current density at the same applied potential. This result underscores the importance of assembling catalytically active materials and nanocarbon at the molecular level in designing high-performing electrochemical catalysts.

From N_2 adsorption–desorption isotherms shown in the Supporting Information, Figure S6, it is clear that the specific surface area of FeNi-GO LDH ($104.96\ sq\,m\,g^{-1}$) is much larger than those of FeNi LDH/GO ($77.165\ sq\,m\,g^{-1}$), FeNi LDH + GO ($65.48\ sq\,m\,g^{-1}$), and FeNi LDH ($55.135\ sq\,m\,g^{-1}$). Therefore, the high electrochemical catalytic performance of FeNi-GO LDH could be partly attributed to 1) the large exposed FeNi hydroxide surfaces stemming from its unique layered structure, and 2) the GO layers that serve to finely divide the FeNi double hydroxide layers to further increase the exposed catalytic active sites.

To further improve electrochemical performances of the catalysts, the assembled GOs at the interlayers of FeNi LDHs were reduced by a chemical method.[13] The XPS spectrum of the reduced GO (rGO) and FeNi double hydroxide (FeNi-rGO LDH) hybrid is in general consistent with that of FeNi-GO LDH (Supporting Information, Figure S5A), indicating that the chemical structure of the LDH hybrid is largely maintained. Comparing with the C 1s core-level spectrum of FeNi-GO LDH (Figure 2B), however, the deconvoluted C 1s core-level spectrum of FeNi-rGO LDH (Supporting Information, Figure S5C) shows that the concentration of oxidized species decreased, whereas the amount of sp^2 hybridization increased. This confirms that the chemical reduction of GO in the interlayers between the FeNi double hydroxide layers was indeed successful. Moreover, from an XRD pattern (Supporting Information, Figure S7), the (003) and (006) diffraction peaks of FeNi-rGO LDH are retained, indicating that the layered structure is unchanged. Moreover, compared with FeNi-GO LDH, the two peaks of FeNi-rGO are shifted to somewhat larger 2θ values, indicating that the basal spacing of FeNi-rGO LDH is slightly smaller than that of FeNi-GO LDH, in agreement with the generally smaller thickness of rGO than that of GO. When the FeNi-rGO LDH was used to catalyze the OER (see the LSV curve in Figure 3A), the current density spiked at 1.425 V, indicating the start of the catalytic water oxidation at the overpotential of around 0.195 V. Note that this overpotential is lower than that of the FeNi-GO LDH catalyst, highlighting the much enhanced OER activity of the FeNi-rGO LDH hybrid because of the improved charge transport owing to the embedded rGO layers. From the AC impedance spectra of FeNi LDH and FeNi-rGO LDH (Supporting Information, Figure S8), it is clear that at the potential of 1.40 V (close to the OER onset potential; Supporting Information, Figure S8A), the electron transference resistance on the surface of FeNi-rGO LDH is slightly smaller than that on FeNi LDH. When the potential was increased to 1.48 V (corresponding to an overpotential of 0.25 V; Supporting Information, Figure S8B), the Nyquist plots of both materials showed much smaller semicircle diameters, indicating the electron transfer in both materials becomes much faster than that at 1.40 V. More importantly, FeNi-rGO LDH affords a much smaller electron transference resistance than FeNi LDH, suggesting that the assembly of rGO with FeNi double hydroxides at the molecular level facilitates the charge transference that contribute to a superior electrochemical performance for water splitting.

The potential required to achieve a current density of 10 $mA\,cm^{-2}$ is an important performance index of an OER catalyst because it is approximately the current density for a 10% efficient solar-to-fuel conversion device.[3b,14] Here for our OER catalysts of FeNi-rGO LDH hybrid, FeNi-GO LDH, FeNi LDH/GO, FeNi LDH + GO, and FeNi LDH, the corresponding potentials at 10 $mA\,cm^{-2}$ were 1.436, 1.451, 1.459, 1.465, and 1.462 V, respectively (Figure 3B). Several remarks on the result are required. First, for the OER catalysts obtained by simply mixing with GO or even without any nanocarbon, a higher voltage was required to achieve 10 $mA\,cm^{-2}$, and this confirms that the synergetic effect arising from the interactions between the catalysts and the underlying nanocarbon could improve the electrocatalytic performance. Second, these values are much lower than those of the reported earth abundant OER catalysts[3b–d] and comparable to that of IrO_x (0.32 ± 0.04 V).[3b,15] Finally, the activity of the FeNi-rGO LDH hybrid catalyst is the highest among the samples we prepared in this work and its

performance stability is also remarkable (Figure 3C). In fact, it outperformed the reported earth-abundant metal hydroxide OER catalysts[3b,c] at higher current densities; for example, 10 mA cm^{-2} and 20 mA cm^{-2}, by the lower required overpotentials (Figure 3C). The high current density was resulted from the high OER catalytic activity of FeNi LDHs, because bare rGO exhibited little current density under the potential lower than 1.5 V (Figure 3D). Furthermore, the FeNi-rGO LDH showed a nearly constant operating potential at around 1.455 V for about 8 h when biased galvanostatically at 10 mA cm^{-2} (Supporting Information, Figure S9). Moreover, the FeNi-rGO LDH maintained nearly the same OER onset potentials and the similar LSV curve after the chronopotentiometry measurement for 8 h (Figure 3D).

The Tafel slope, which describes the influence of potential, or overpotential on steady-state current density, is an important factor for the evaluation of OER kinetics. Tafel data of the as prepared FeNi LDH-based catalysts on OER were collected and are presented in Figure 4A. Impressively,

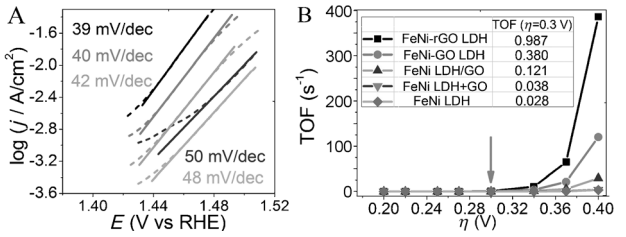

Figure 4. Steady-state Tafel measurement and turnover frequencies for FeNi-based catalysts. A) Tafel plots of OER catalyzed by (top to bottom) FeNi-rGO LDH, FeNi-GO LDH, FeNi LDH/GO, FeNi LDH + GO, and FeNi LDH. B) TOF values of the catalysts as a function of overpotential. The arrow indicates the TOF values at an overpotential of 0.3 V (see inset table). All measurements were conducted with a catalyst loading of 0.25 mg cm^{-2} on Ni foam electrodes and the data were recorded at 0.1 mV s^{-1} in 1 M KOH.

the estimated Tafel slopes of these catalysts are close to those of the well-established OER catalysts IrO_2 (ca. 49 mV/dec)[4d,6] and Ir/C (ca. 40 mV/dec).[3c,16] Within the catalyst series, the OER activity increased in the order of FeNi-rGO LDH (39 mV/dec) < FeNi-GO LDH (40 mV/dec) < FeNi LDH/GO (42 mV/dec) < FeNi LDH (48 mV/dec) < FeNi LDH + GO (50 mV/dec). This closely parallels the LSV result (Figure 3A) that the FeNi-GO LDH and FeNi-rGO LDH hybrids exhibit higher current densities than the others at the same applied potential, and manifests again the decreased charge-transfer resistance owing to the insertion of the graphene nanosheets. Therefore, the Tafel result lends further support to the conclusion that the advanced catalytic performances of the FeNi-graphene LDH on OER is derived from the strong interactions between the FeNi double hydroxide layers and the graphene layers at the molecular level. Moreover, on the basis of the assumption that all of the metal ions in the catalysts were involved in the electrochemical reaction,[3c,d] the OER turnover frequencies (TOFs) at different overpotentials were calculated and plotted in Figure 4B. It should be pointed out that the as calculated TOFs could be gross underestimations of the actual TOFs because not every metal atom could be catalytically active. Nevertheless, even with these overly conservative estimations, the TOF of FeNi-rGO LDH hybrid is still respectable, and it showed a clear increase with overpotential that was higher than that of other catalysts under the same applied potentials (see Figure 4B). Moreover, it is worth noting that the TOF values of the FeNi-rGO LDH hybrid at an overpotential of 0.3 V is close to 1 s^{-1}, much higher than the previously reported LDH based catalysts.[3b–d,6]

In conclusion, we have assembled an OER hybrid catalyst by alternately stacking the FeNi double hydroxide cation layers with the negatively charged GO layers. This hybrid combines the high OER catalytic activity of the FeNi double hydroxide with the charge conducting graphene layers synergistically. The as-prepared FeNi-GO and FeNi-rGO LDH hybrids exhibited advanced electrocatalytic activity and stability on OER in alkaline solution. The overpotential of catalytic OER is among the lowest of non-noble metal catalysts (as low as 0.195 V) and the Tafel slope is close to the Ir/C catalyst at 40 mV/dec.[16] The high catalytic performance is mainly attributed to the intrinsic catalytic activity of the FeNi double hydroxide layers. However, the strong interactions of the FeNi double hydroxide with the assembled rGO finely divided the LDH layers alternately, which assisted in exposing the catalytically active sites, improved the charge transport through the rGO layers, and thus led to the optimal OER performance. This work offers a novel strategy at molecular level to design low-cost OER electrocatalysts that could outperform noble-metal-based electrocatalysts in alkaline solutions, and will inspire the development of renewable energy sources.

Received: February 26, 2014
Published online: June 6, 2014

Keywords: electrochemical catalyst · FeNi · graphene · layered double hydroxide · oxygen evolution reaction

[1] D. Galizzioli, F. Tantardini, S. Trasatti, *J. Appl. Electrochem.* **1974**, *4*, 57–67.
[2] a) J. Suntivich, K. J. May, H. A. Gasteiger, J. B. Goodenough, Y. Shao-Horn, *Science* **2011**, *334*, 1383–1385; b) J. O. Bockris, T. Otagawa, *J. Phys. Chem.* **1983**, *87*, 2960–2971.
[3] a) R. D. Smith, M. S. Prévot, R. D. Fagan, Z. Zhang, P. A. Sedach, M. K. J. Siu, S. Trudel, C. P. Berlinguette, *Science* **2013**, *340*, 60–63; b) C. C. McCrory, S. Jung, J. C. Peters, T. F. Jaramillo, *J. Am. Chem. Soc.* **2013**, *135*, 16977–16987; c) M. Gong, Y. Li, H. Wang, Y. Liang, J. Z. Wu, J. Zhou, J. Wang, T. Regier, F. Wei, H. Dai, *J. Am. Chem. Soc.* **2013**, *135*, 8452–8455; d) X. Zou, A. Goswami, T. Asefa, *J. Am. Chem. Soc.* **2013**, *135*, 17242–17245; e) P. Liu, Y. J. Guan, R. A. van Santen, C. Li, E. J. M. Hensen, *Chem. Commun.* **2011**, *47*, 11540–11542; f) C. G. Silva, Y. Bouizi, V. Fornes, H. Garcia, *J. Am. Chem. Soc.* **2009**, *131*, 13833–13839; g) D. K. Bediako, Y. Surendranath, D. G. Nocera, *J. Am. Chem. Soc.* **2013**, *135*, 3662–3674; h) L. Wang, D. Wang, X. Y. Dong, Z. J. Zhang, X. F. Pei, X. J. Chen, B. Chen, J. Jin, *Chem. Commun.* **2011**, *47*, 3556–3558.
[4] a) I. C. Man, H. Y. Su, F. Calle-Vallejo, H. A. Hansen, J. I. Martinez, N. G. Inoglu, J. Kitchin, T. F. Jaramillo, J. K. Norskov, J. Rossmeisl, *ChemCatChem* **2011**, *3*, 1159–1165; b) J. Ross-

meisl, Z. W. Qu, H. Zhu, G. J. Kroes, J. K. Norskov, *J. Electroanal. Chem.* **2007**, *607*, 83 – 89; c) J. O. Bockris, T. Otagawa, *J. Electrochem. Soc.* **1984**, *131*, 290 – 302; d) S. Trasatti, *J. Electroanal. Chem.* **1980**, *111*, 125 – 131.

[5] T. A. Betley, Q. Wu, T. Van Voorhis, D. G. Nocera, *Inorg. Chem.* **2008**, *47*, 1849 – 1861.

[6] L. Trotochaud, J. K. Ranney, K. N. Williams, S. W. Boettcher, *J. Am. Chem. Soc.* **2012**, *134*, 17253 – 17261.

[7] M. Wehrens-Dijksma, P. Notten, *Electrochim. Acta* **2006**, *51*, 3609 – 3621.

[8] a) K. I. Bolotin, K. J. Sikes, J. Hone, H. L. Stormer, P. Kim, *Phys. Rev. Lett.* **2008**, *101*, 096802; b) A. A. Balandin, S. Ghosh, W. Z. Bao, I. Calizo, D. Teweldebrhan, F. Miao, C. N. Lau, *Nano Lett.* **2008**, *8*, 902 – 907; c) C. Lee, X. D. Wei, J. W. Kysar, J. Hone, *Science* **2008**, *321*, 385 – 388.

[9] a) R. kumar Allada, A. Navrotsky, H. T. Berbeco, W. H. Casey, *Science* **2002**, *296*, 721 – 723; b) Z. Liu, R. Ma, M. Osada, N. Iyi, Y. Ebina, K. Takada, T. Sasaki, *J. Am. Chem. Soc.* **2006**, *128*, 4872 – 4880.

[10] N. Iyi, T. Matsumoto, Y. Kaneko, K. Kitamura, *Chem. Mater.* **2004**, *16*, 2926 – 2932.

[11] a) J. Zheng, H. Zhang, S. Dong, Y. Liu, C. T. Nai, H. S. Shin, H. Y. Jeong, B. Liu, K. P. Loh, *Nat. Commun.* **2014**, *5*, 2995; b) L. Peng, X. Peng, B. Liu, C. Wu, Y, Xie, G. Yu, *Nano Lett.* **2013**, *13*, 2151.

[12] a) C. Mattevi, G. Eda, S. Agnoli, S. Miller, K. A. Mkhoyan, O. Celik, D. Mastrogiovanni, G. Granozzi, E. Garfunkel, M. Chhowalla, *Adv. Funct. Mater.* **2009**, *19*, 2577 – 2583; b) T.-K. Hong, D. W. Lee, H. J. Choi, H. S. Shin, B.-S. Kim, *ACS Nano* **2010**, *4*, 3861 – 3868; c) F. Tristán-López, A. Morelos-Gomez, S. M. Vega-Díaz, M. L. Garcia-Betancourt, N. Perea-Lopez, A. L. Elias, H. Muramatsu, R. Cruz-Silva, S. Tsuruoka, Y. A. Kim, *ACS Nano* **2013**, *7*, 10788 – 10789.

[13] D. Li, M. B. Mueller, S. Gilje, R. B. Kaner, G. G. Wallace, *Nat. Nanotechnol.* **2008**, *3*, 101 – 105.

[14] M. G. Walter, E. L. Warren, J. R. McKone, S. W. Boettcher, Q. Mi, E. A. Santori, N. S. Lewis, *Chem. Rev.* **2010**, *110*, 6446 – 6473.

[15] Y. Zhao, E. A. Hernandez-Pagan, N. M. Vargas-Barbosa, J. L. Dysart, T. E. Mallouk, *J. Phys. Chem. Lett.* **2011**, *2*, 402 – 406.

[16] S. Trasatti, G. Lodi, *Electrodes of Conductive Metallic Oxides*, Elsevier, Amsterdam, **1981**.

